Effects of Internal Na^+ on the Ca Channel Outward Current in Mouse Neoplastic B Lymphocytes

NAOHIDE YAMASHITA, SERGIO CIANI, and SUSUMU HAGIWARA[†]

From the Department of Physiology, Jerry Lewis Neuromuscular Research Center and Ahmanson Laboratory of Neurobiology in the Brain Research Institute, University of California School of Medicine, Los Angeles, California 90024

ABSTRACT The whole-cell configuration of the patch-clamp technique was used to study the outward Na^+ current through Ca channels in hybridoma cell lines (202B and 206), constructed by fusion of S194 myeloma cells with murine splenic B lymphocytes. The concentration of Na^+ in the electrode solution, $[Na^+]_p$, was changed by isosmotic replacement of Na^+ with *N*-methyl-D-glucamine$^+$ ions. When 2.5 mM calcium was present in the bath, neither the current nor the reversal potential was significantly altered by changes in the level of external Na^+ ($[Na^+]_o$. By contrast, both of those properties were strongly affected by $[Na^+]_p$. At fixed depolarizing potentials, the outward current increased approximately as the square power of $[Na^+]_p$, a feature that cannot be easily explained by one-ion models for a channel or by "continuum" theories based on electrodiffusion. Instead, all the data could be well described by a "single-file" model for a two-site pore that admits up to two ions. Although double occupancy of the Ca channel by divalent cations has been proposed previously (Hess and Tsien. 1984. *Nature.* 309: 453–456; Almers et al., 1984. *J. Physiol.* 353: 585–608), this study indicates that, in our system, states of the channel with two Na^+ ions must also be considered in order to explain the dependence of the outward current on $[Na^+]_p$. A good fit to the data could be obtained by assuming that both sites in the channel are "electrically" close to its cytoplasmic end and that most of the voltage dependence pertains to the rates for ion exit to the external medium. The values of the parameters suggest that: (*a*) Ca^{2+} is bound most strongly by the site nearest to the cytoplasm (in both singly and doubly occupied channels); (*b*) in channels with two Ca^{2+} ions, the dissociation constant of the site close to the external mouth must be >2.5 mM; and (*c*) in pores occupied by two Na^+ ions, the rate constant for Na^+ exit to the external solution is larger than the rate constant for Na^+ exit to the cytoplasm.

[†]Professor Hagiwara died just before submission of this paper.

Address reprint requests to Dr. Naohide Yamashita, Department of Physiology, Jerry Lewis Neuromuscular Research Center, UCLA School of Medicine, Los Angeles, CA 90024.

J. GEN. PHYSIOL. © The Rockefeller University Press · 0022-1295/90/09/0559/21 $2.00
Volume 96 September 1990 559–579

INTRODUCTION

Recent studies have shown that monovalent cations are capable of carrying inward current through Ca^{2+} channels when the extracellular concentration of Ca^{2+} is decreased to micromolar levels, thus suggesting the presence in the channel of binding sites for Ca^{2+} with a dissociation constant of the same order of magnitude (Kostyuk and Krishtal, 1977; Kostyuk et al., 1983; Almers et al., 1984; Fukushima and Hagiwara, 1985). However, earlier reports indicated that the inward Ca^{2+} current, far from saturating at micromolar levels of external Ca^{2+}, is still an increasing function of the concentration of external Ca^{2+} even in the millimolar range (Hagiwara and Takahashi, 1967; Hagiwara and Byerly, 1981). One way to reconcile these findings has been to propose that Ca channels are multi-ion pores (Almers and McCleskey, 1984; Hess and Tsien, 1984), a hypothesis that is also strengthened by independent evidence. For example, Hess and Tsien (1984), using ventricular cells from mammalian heart, have shown that the conductance in mixtures of Ca^{2+} and Ba^{2+} exhibits anomalous mole-fraction dependence with sharp minima at low fractions of Ca^{2+}, and similar features have also been described in the Ca channels from Lymnea neurons (Byerly et al., 1985). As it is known, anomalous mole-fraction dependence of the conductance is inconsistent with one-ion channels with fixed energy profiles, but can be explained by single-file pores (Hille and Schwarz, 1978).

While inward currents carried by monovalent cations through Ca channels can be detected only when the external Ca^{2+} concentration is of the order of 1 μM or less, outward currents carried by monovalent cations through the same channel can be observed also at physiological Ca^{2+} levels if the applied potential is stepped to sufficiently high positive values (Reuter and Scholz, 1977; Fenwick et al., 1982; Almers et al., 1984; Fukushima and Hagiwara, 1985; Iijima et al., 1986; Campbell et al., 1988). However, while the characteristics of the inward current have been studied in many systems, the outward current has not been analyzed in detail, and little attention has been given to the information that it may give about the permeation properties of the channel.

Applying the whole-cell configuration of the patch clamp technique to cells from a hybridoma cell line, this study describes the effects on the channel electrical properties of varying both the internal and external concentrations of Na^+, and also formulates a model based on Eyring rate theory in order to interpret the experimental results. It is concluded that a good fit to the data demands fairly rigid constraints upon the position in the electric field of the peaks and wells of the energy barriers, which are similar to those determined in a previous study (Iijima et al., 1986), and also requires that a state of the channel with double occupancy by Na^+ be included in the kinetics, along with states with double occupancy by Ca^{2+} and mixed ions. A preliminary report of this work has already been published as an abstract (Yamashita et al., 1989).

METHODS

Materials

Two hybridoma cell lines (202B and 206), constructed by fusion of S194 mouse myeloma cells with mouse splenic B lymphocytes and known to secrete immunoglobulin M, were used in the

experiments. The culture was kept at 37°C in RPMI 1640 medium supplemented with 10% fetal calf serum, and subculture was done every 4 d. The cells were used for the electrophysiological experiments 3 or 4 d after renewal of the medium, since it had previously been found that maximal Ca^{2+} current was obtained at that stage of growth (Fukushima et al., 1984). The cell diameter was ~20 μm.

Electrophysiological Analysis

The whole-cell configuration of the patch clamp technique was used in the electrophysiological studies. The resistance of the patch electrode ranged from 3 to 8 MΩ and the seal resistance was 10–30 GΩ. The holding membrane potential was −94 to −96 mV, a potential at which the inactivation of the Ca channel was completely removed. The current was filtered through a low-pass filter at 1 kHz, and the steady leakage current was subtracted. Other details of the technique were essentially similar to those reported previously (Fukushima and

TABLE I

Compositions of the Solutions Millimolar

	External solutions						
	Na^+	Ca^{2+}	Mg^{2+}	K^+	EDTA	choline	Cl^-
Standard	130.3	2.5	1.0	5.0	0	0	143.3
26 mM Na	26.0	2.5	1.0	5.0	0	104.3	143.3
Ca^{2+}-, Mg^{2+}-, K^+-free EDTA	144.3	0	0	0	2.0	0	135.3

All media contained 17 mM glucose and pH was adjusted at 7.4 by 10 mM HEPES (Na salt). In EDTA-containing solution pH was adjusted by adding NaOH in addition to 10 mM HEPES Na. Na^+ concentration also includes the amount added for titrating HEPES and EDTA.

	Internal solutions					
X	Cl^-	Aspartic acid	ATP-Na	$MgCl_2$	EGTA	HEPES
156	40	95	2	1	5	10

X = Na + *N*-methyl-D-glucamine. X concentration also includes the amount added for titrating HEPES and EGTA, and the amount of salt of ATP. The pH was adjusted at 7.3.

Hagiwara, 1985). The composition of the solutions is shown in Table I. The pH of the extracellular media was adjusted to 7.4 and that of the intracellular medium to 7.3. Corrections of the membrane potential to compensate for liquid junction potentials were made as described by Hagiwara and Ohmori (1982). All the experiments were carried out at room temperature (20–25°C).

It has been previously demonstrated that Ca channels are the only type of voltage-gated channels present in hybridoma cell lines secreting immunoglobulin, and that there is probably one type of Ca channel with voltage-dependent inactivation (Fukushima et al., 1984; Fukushima and Hagiwara, 1985). This property is characteristic of the type I (or transient type) Ca channels, which are found also in other tissues (Hagiwara et al., 1975; Nowycky et al., 1985; Narahashi et al., 1987). However, in ~30% of the cells in the 202B cell line it was noticed that a slowly inactivating Ca^{2+} current was superimposed upon that of the type I Ca^{2+} channels. This slowly inactivating Ca^{2+} current, which resembled that of the type II (or long-lasting) Ca channels, appears to be a peculiar property of the 202B clone, since it was almost never observed in the 206 cell line, and was also absent in related clones (MAb2-1 and MAb-7B) studied previously (Fukushima et al., 1984; Fukushima and Hagiwara, 1985). Since

the objective of this study was to examine the outward current carried by monovalent cations through the type I Ca channels, cells showing the presence of type II Ca channels were discarded.

RESULTS

Evaluation of the Intracellular Sodium Concentration

Previous work by Fukushima and Hagiwara (1985) reported that the permeabilities of K^+, Rb^+, and Cs^+, referred to Na^+, are: 0.8, 0.6, and 0.35, respectively. In this work, the effect of the intracellular concentration of monovalent cations on the

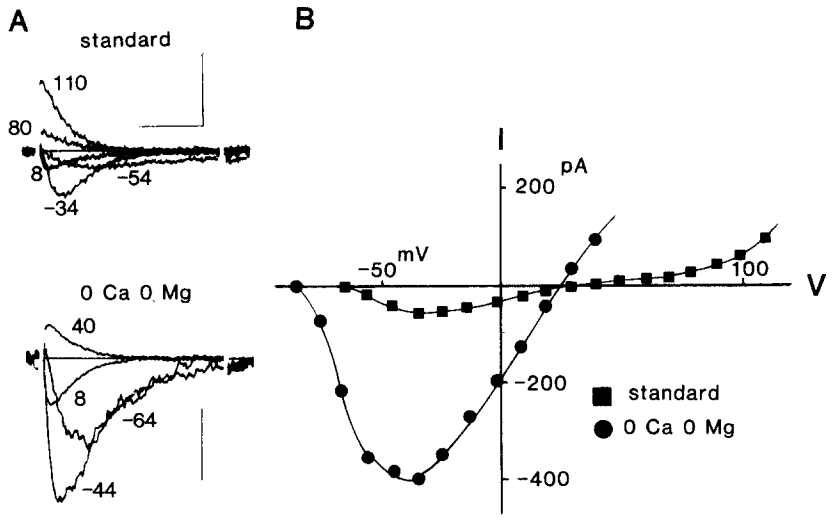

FIGURE 1. Ca^{2+} channel currents in the standard and in Ca^{2+}-, Mg^{2+}, K^+-free medium. The upper panel in *A* shows the Ca^{2+} channel currents recorded in the standard extracellular medium; the lower panel shows those recorded in the Ca^{2+}-, Mg^{2+}-, K^+-free medium containing 2 mM EDTA. The patch electrode solution contained 50 mM Na^+. Both records refer to the same cell. Holding potential was −96 mV and the test potentials (in millivolts) are indicated in the figures. Time scale (horizontal) and current amplitude (vertical) bars in the upper panel are equal to 50 ms and 100 pA, respectively. Current amplitude bar in the lower panel is equal to 200 pA. Time scale in the lower panel is the same as that in the upper panel. *B* shows the *I-V* relationships of the records in *A*. Squares indicate the *I-V* relationship in the standard medium and circles, that in Ca^{2+}-, Mg^{2+}-, K^+-free medium.

outward current was studied by dialyzing the interior of the cell with Na^+, the most permeant of the alkali cations. In standard conditions, the solution of the patch pipette contained 156 mM Na^+ and 0 K^+, changes in the concentrations of Na^+ being obtained by partial replacement with the impermeant ion, *N*-methyl-D-glucamine$^+$. Data recording generally started 5 min after establishment of the whole-cell clamp conditions. In conditions of complete dialysis, the sodium concentration inside the cell, $[Na^+]_i$, would be expected to be the same as in the pipette,

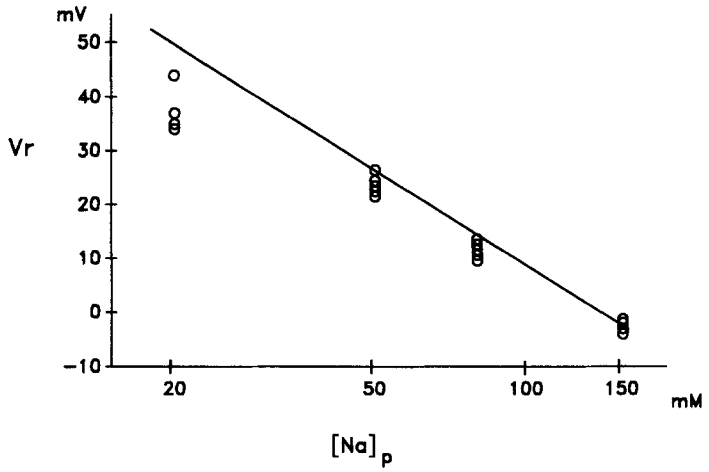

FIGURE 2. The relationship between the reversal potential and the concentration of Na^+ in the patch electrode solution ($[Na^+]_p$) for cells exposed to the Ca^{2+}-, Mg^{2+}-, K^+-free medium containing 2 mM EDTA. The ordinate indicates the reversal potential and the abscissa $[Na]_p$ on a logarithmic scale. Each point represents the datum from a single cell. The straight line was drawn according to the Nernst equation.

$[Na^+]_p$. To test whether this was the case, after recording the data with the standard extracellular medium, the external medium was exchanged with a Ca^{2+}-, Mg^{2+}-, and K^+-free medium containing 2 mM EDTA and 144.3 mM Na^+. Since Na^+ should be the sole permeant ion present in these conditions, the reversal potential would be expected to obey the Nernst equation for this ion. While many cells deteriorated in the Ca^{2+}-free solution, successful recordings could be obtained in ~20% of them. Fig. 1 *A* shows the current records obtained with the standard external medium (upper panel) and those obtained from the same cell when that medium was replaced with the Ca^{2+}-free solution defined above (lower panel). $[Na^+]_p$ in the pipette was 50 mM. The corresponding relationships between the voltage and the peak current (*I-V* relationships) are illustrated in Fig. 1 *B*. In Fig. 2, the reversal potential, V_r, recorded in the Ca^{2+}-, Mg^{2+}-, K^+-free medium containing Na^+ as the sole permeant

TABLE II

Average Values of V_r and $[Na^+]_i$ for $[Na^+]_p$

$[Na^+]p$	V_r	$[Na^+]_i$	n
mM	*mV*	*mM*	
156	−2.3 ± 1.2*	153 ± 8.8*	4
80	11.4 ± 1.5	92 ± 5.7	6
50	23.7 ± 1.9	55 ± 4.1	5
20	37.3 ± 4.7	33 ± 5.6	4

*Mean ± standard deviation. $[Na^+]_p$ indicates the Na^+ concentration in the patch electrode solution, V_r, the reversal potential in Ca^{2+}-, Mg^{2+}-, K^+-free solution, $[Na^+]_i$, the estimated intracellular Na^+ concentration, and n, the number of the examined cells.

ion, is plotted against the logarithm of the sodium concentration in the pipette solution, $[Na^+]_p$. If the dialysis had been complete, the data should fall on a straight line with a slope of 58 mV for a 10-fold change in $[Na^+]_p$. While most of the data follow this prediction, some deviations are seen in the range of low $[Na^+]_p$, as if the actual intracellular Na^+ concentration were higher than that expected in the case of thorough dialysis. At least two reasons may account for these two small discrepancies: (*a*) some amounts of K^+ may remain in the cell due to incomplete dialysis; and (*b*) *N*-methyl-D-glucamine$^+$ may be slightly permeant. Also, some inaccuracy in the measurements of V_r at low internal Na^+ concentrations cannot be excluded. The averaged values of V_r and the estimated values of $[Na^+]_i$ for different Na^+ concentrations in the pipette, $[Na^+]_p$, have been listed in Table II. In this paper we shall use $[Na^+]_p$ to denote the intracellular Na^+ concentration, because $[Na^+]_p$ is a known quantity and because the differences between $[Na^+]_p$ and the calculated values of $[Na^+]_i$ are not large.

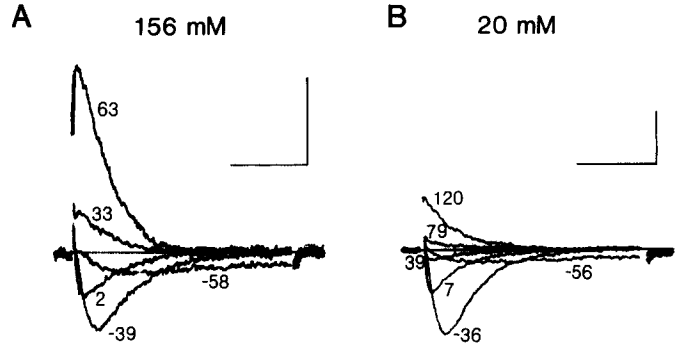

FIGURE 3. Effects of the internal Na^+ concentration on the membrane current. *A*, Membrane currents recorded using the standard external medium and the standard patch electrode solution with 156 mM Na^+. *B*, Membrane currents recorded in the standard external medium with the patch electrode solution containing 20 mM Na^+. Time scale (horizontal) and current amplitude (vertical) bars are equal to 50 ms and 100 pA, respectively, in both *A* and *B*. The holding potential was −96 mV and test potentials (in millivolts) are indicated in the figure in both *A* and *B*. The reversal potentials were +25 mV in *A* and +59 mV in *B*, respectively.

Effects of Internal Na^+ on the Reversal Potential

Fig. 3, *A* and *B* illustrate the membrane current obtained in two different cells. $[Na^+]_p$ was 156 mM in one of them (standard), 20 mM in the other. The membrane potential at which the inward current became apparent was almost identical in the two records. Fig. 4 plots the time-to-peak and the inactivation time constant that correspond to the currents in Fig. 3. There is almost no difference in this parameter between the two cells, indicating that changes in $[Na^+]_p$ have negligible effects on the kinetics of gating. However, one discrepancy between the records of Fig. 3, *A* and *B* was the value of the reversal potential V_r, which was +25 mV in *A* and +59 mV in *B*.

The relation between V_r and $[Na^+]_p$, determined in standard external medium, is displayed in Fig. 5. The continuous line in Fig. 5 represents a fit to the data with a "two-site, two-ion" model for the Ca channel, as will be described later.

Dependence of the Amplitude of the Outward Current on $[Na^+]_p$

Since the amplitude of the membrane current varied considerably from cell to cell, the current amplitude of each cell was normalized to the peak value of its inward current to allow comparison of the data from different experiments. The current–

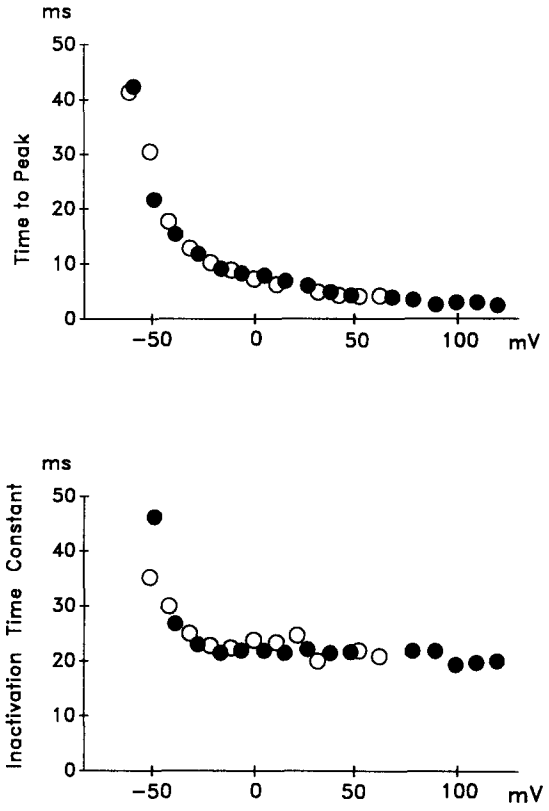

FIGURE 4. Time to peak (upper panel) and the inactivation time constant (lower panel) of Ca^{2+} current. Data were obtained from the cells shown in Fig. 3. Open circles indicate the data of the cell with the internal solution containing 156 mM Na^+ and solid circles indicate the data of the cell with the internal solution containing 20 mM Na^+.

voltage (*I-V*) relationships of representative cells, corresponding to internal solutions with different Na^+ concentrations, are displayed in Fig. 6, where each point represents the mean current normalized according to the criterion just mentioned. The outward current increased with the level of internal sodium, as shown in Fig. 7, where the current amplitude at +65 mV is plotted against $[Na^+]_p$. An uncommon feature of this plot is that the dependence is more steep than linear, such that it could be fitted by a function proportional to a power of $[Na^+]_p$ with an exponent greater than one. It was thought at first that this effect might be explained, at least in part, by changes in the interaction between the Ca^{2+} and Na^+ fluxes consequent to

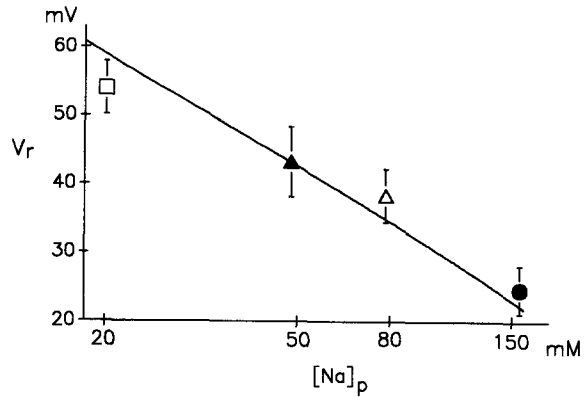

FIGURE 5. Relationship between the reversal potential in the standard external medium and the internal Na^+ concentration ($[Na]_p$). The ordinate indicates the value of the reversal potential and the abscissa that of $[Na]_p$ on a logarithmic scale. Symbols indicate mean reversal potentials and bars indicate standard deviations. The numbers of the cells examined are 28 with 156 mM $[Na^+]_p$, 17 with 80 mM $[Na^+]_p$, 7 with 50 mM $[Na^+]_p$, and 13 with 20 mM $[Na^+]_p$. The continuous line is the theoretical fit with the model.

changes in the level of sodium in the pipette. For example, raising the level of $[Na^+]_p$ might cause (by extruding Ca^{2+} from the channel at positive voltages) such a drastic decrease of the inward flux of Ca^{2+} that the combined effect of this decrease and of the concomitant increase in the outward flux of Na^+ would result into an unusually steep dependence of the outward current on $[Na^+]_p$. However, in the experiments where 2.5 mM Ca^{2+} was present in the external medium and *N*-methyl-D-glucamine$^+$ was the sole monovalent cation in the pipette, no inward current could be measured above +50 mV (data not shown), a result that is inconsistent with the argument presented above, since it implies that no further decrease of the inward current should be expected beyond that voltage.

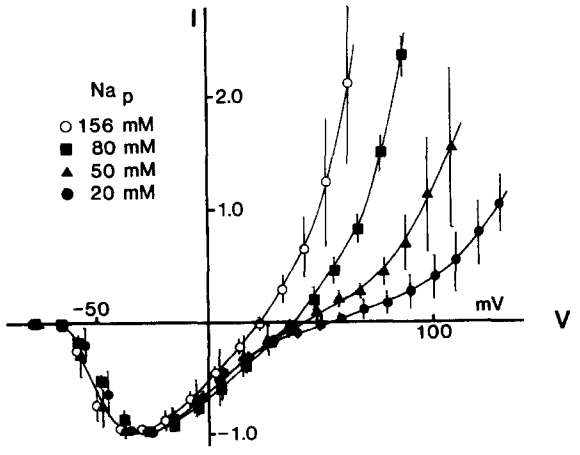

FIGURE 6. Normalized *I-V* relationships of the membrane current recorded with various concentrations of intracellular Na^+. Membrane currents were normalized by dividing all currents by the maximum amplitude of the peak inward current for each cell. Open circles (six cells), solid squares (four cells), solid triangles (four cells), and solid circles (four cells) refer to the following values of $[Na^+]_p$: 156, 80, 50, and 20 mM, respectively. All data were obtained with standard extracellular medium. The holding potential was between −94 and −96 mV. Vertical bars indicate standard deviations and Na_p is the Na^+ concentration in the patch electrode solution. Continuous lines were drawn by eye.

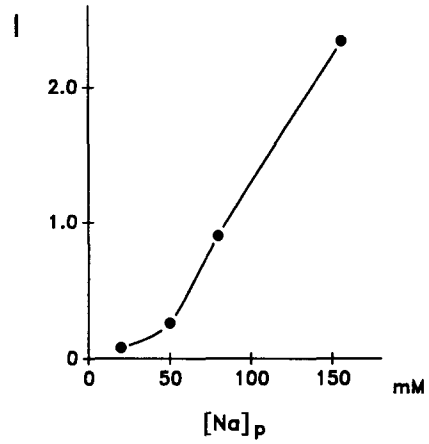

FIGURE 7. Relationship between the amplitude of normalized outward current at +65 mV and the $[Na^+]_p$. The data were taken from Fig. 6 and the continuous line was drawn by eye.

Effect of External Na^+ on the Current

Previous work has demonstrated that, when $[Na^+]_p$ was 156 mM, eliminating Na^+ from the external solution resulted in very little effect on either V_r or the amplitude of the outward current (Fukushima and Hagiwara, 1985). The same conclusion can be drawn from our experiments, in which different values of $[Na^+]_p$ were also tested. Fig. 8 displays two *I-V* curves, corresponding to $[Na^+]_o$ = 130.3 mM (standard solution) and $[Na^+]_o$ = 26 mM, respectively, with $[Na^+]_p$ = 50 mM in both cases. As can be seen, changes in V_r and in the current are very minor, similar results having also been obtained from experiments with different values for $[Na^+]_p$.

A Two-Site, Two-Ion Model for Ca^{2+} Channels

On the basis of the existing evidence that Ca channels are multi-ion pores, the *I-V* data were fitted using a two-site, single-file model for a channel, which is similar in many respects to a model formulated previously by Urban and Hladky (1979). As is known, nine states of occupancy of the pore are possible if two permeant species are present, and a system with the same number of equations is required to calculate the probabilities of these states and the ion fluxes. Assuming that Ca^{2+} and Na^+ are the

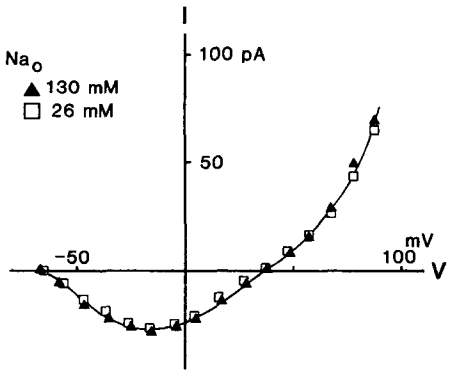

FIGURE 8. Effect of extracellular Na^+ concentration on the membrane current. Triangles refer to the data recorded with standard extracellular medium ($[Na^+]_o$ = 130.3 mM); squares refer to the case of 26 mM Na^+ in the external medium using the same cell. $[Na^+]_p$ was 156 mM in both records. Holding potential was −94 mV.

only permeant ions, the nine states of the channel that are consistent with our model are those shown and numbered in Fig. 9 *B*. Once the probabilities of states 2, 3, 5, and 6 are evaluated, the total fluxes of Ca^{2+} and Na^+ are given by

$$j_{Ca} = \lambda'_{Ca} P_2 - \lambda''_{Ca} P_3 \quad (1)$$

$$j_{Na} = \lambda'_{Na} P_5 - \lambda''_{Na} P_6, \quad (2)$$

where the λ's denote rate constants for crossing the middle barrier in singly occupied channels, and the indices ′ and ″ (when applied to rate constants) indicate outward and inward movement, respectively.

The general solution for the steady-state electric current through a single-file, two-site channel has been given by Urban and Hladky (1979). Although the results can be written compactly by grouping lengthy terms, the complete kinetic scheme implies 22 independent rate constants, in addition to other parameters in the form

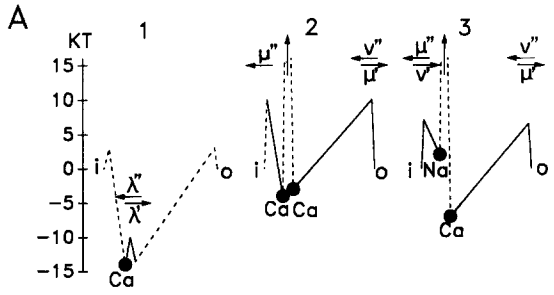

B

IN	1	2	3	4	5	6	7	8	9
	0	Ca	0	Ca	Na	0	Na	Na	Ca
OUT	0	0	Ca	Ca	0	Na	Na	Ca	Na

FIGURE 9. A two-site, two-ion model for the Ca^{2+} channel. *A*, Approximate energy profile for three occupancy states of the channel. (No absolute value for energy peaks or wells is deducible from the fitting parameters.) Dashed lines in each profile refer to forbidden transitions for the particular state of occupancy shown in that profile. Diagram also illustrates the hypothesis, demanded by the fit, the most of the voltage dependence pertains to the rate constants for exit to the external medium, μ′. *B*, States of occupancy of a two-site, two-ion channel permeable to both Na^+ and Ca^{2+}. Empty sites are indicated by 0.

of "electrical distances" of the peaks and the wells of the energy profiles. It is thus clear that the use of this model to fit the data generally available for biological channels may become practical only if suitable approximations are permitted.

In our development, the only simplification adopted at the outset was the assumption that the probability of the empty state of the channel is negligible, implying that the channel is always occupied by either one or two ions. Thus, when the pore contains only one ion, this will be able to move between the two internal sites, but will not leave the channel before another ion occupies the site that is still vacant. Although this hypothesis will be discussed later, one can intuitively appreciate its reasonableness in view of the widely accepted notion that Ca^{2+} ions bind to Ca^{2+} channels very strongly, and considering that the level of the external Ca^{2+} in our experiments was more than three orders of magnitude higher than the dissociation constant estimated for that binding.

Thus, if the empty state of the channel is neglected, it can easily be seen that the only ions that play a role in our kinetic scheme are ions that enter singly occupied channels, ions that leave doubly occupied channels, and ions that move between the two sites in singly occupied channels. Therefore, all the rate constants for ion entry to the channel and exit from the channel need two indices for proper identification: the lower, for example, to denote the moving ion, the upper to denote the ion that occupies the adjacent site. For example, the rate constant, $\mu_{Ca}^{'Na}$, will describe the jump of a Ca^{2+} ion out of the channel in the external solution when the adjacent site is occupied by one Na^+. Moreover, when a rate constant is voltage dependent, its explicit form, according to Eyring theory, will be given by the product of a voltage-independent term and an exponential of voltage. For example,

$$\mu_{Ca}^{'Na} = \bar{\mu}_{Ca}^{'Na}\, e^{2\Delta\phi}, \tag{3}$$

where $\Delta\phi$ is the potential difference, in units of RT/F, between the site where the ion is located and the peak of the barrier to be crossed, and a bar is used to designate the voltage-independent term in the rate constants. Also, recalling that the rate constants for entering the channel (indicated by ν in Fig. 9 *A*) are proportional to the ion concentrations in the solutions, we shall have

$$\begin{aligned} \nu_{Ca}^{''Ca} &= \rho_{Ca}^{''Ca} C_{Ca}'; & \nu_{Ca}^{''Na} &= \rho_{Ca}^{''Na} C_{Ca}'' \\ \nu_{Na}^{'Na} &= \rho_{Na}^{'Na} C_{Na}'; & \nu_{Na}^{'Ca} &= \rho_{Na}^{'Ca} C_{Na}' \\ \nu_{Na}^{''Na} &= \rho_{Na}^{''Na} C_{Na}''; & \nu_{Na}^{''Ca} &= \rho_{Na}^{''Ca} C_{Na}'', \end{aligned} \tag{4}$$

where the superscripts ′ and ″ on the concentrations refer to the intracellular and external ones, respectively.

Though neglecting the empty state of the channel simplifies the treatment, the explicit equation for the current that is obtained by considering all the other eight states is still too complex for practical use (results not shown in this paper). However, from a comparison between experiments and theory it is possible to infer that such an equation contains many terms that must be very small, and that a further approximation can thus be made. More precisely, the data show that in the presence of 2.5 mM external Ca^{2+}, both the current and the reversal potential are insensitive to even large changes in the level of external Na^+ (26 to 130.3 mM). On the other hand, the theory predicts that effects of external Na^+ on the current and the reversal potential will be negligible only if the probability of the doubly occupied state of the channel with Ca^{2+} in the site close to the intracellular medium and Na^+ in the one close to the external solution (state 9 in Fig. 9 *B*) is very low. Mainly on the basis of these a posteriori arguments we have deemed it justifiable to simplify the treatment by omitting state 9 of the channel from our kinetic scheme. However, as will be argued later in the Discussion, there are also other plausible reasons why, in our system and for our ionic conditions, the probability of state 9 of the channel would be expected to be small compared with that of all the other doubly occupied states.

By neglecting state 9, the expression for the current becomes considerably simpler, although, in order to obtain an equation that is an explicit function of the potential, it is still necessary to select a particular configuration of the channel in

terms of "electrical" distances of the energy peaks and wells. While several possibilities were tried, the only configuration that gave a satisfactory fit to all four sets of *I-V* data in the region of positive potentials in Fig. 6 was the one in which both sites were assumed to be close to the cytoplasmic interface and the peak of the outermost barrier was adjacent to the external end of the channel (see Fig. 9 *A* for an approximate representation of this profile). In this case, the expression for the current (I^N), normalized to its peak value, is found to be

$$I^N = \left\{\frac{P_6 e^{2\phi} C'_{Na}(C'_{Na}e^{\phi} - C''_{Na})}{1 + P_1 e^{\phi}} - \frac{P_7 C''^{\,2}_{Ca}}{1 + P_2 e^{2\phi}}\right\} \times \frac{1}{C''_{Ca}\left[1 + \frac{P_3}{1 + P_2 e^{2\phi}}\right] + [P_4 C''_{Ca} + P_5 e^{2\phi}]\, C'_{Na}}, \quad (5)$$

where $\phi = FV/RT$ (V being the potential difference between the intracellular and extracellular medium), $C'_{Na} = [Na^+]_i$, $C''_{Na} = [Na^+]_o$, and $C''_{Ca} = [Ca^{2+}]_o$, while the exact meaning of the seven parameters will be given in the next section (see the Appendix for a derivation of Eq. 5).

Definition and Physical Meaning of the Parameters in Eq. 5

Since the parameters in Eq. 5 are not all simple quantities, it is helpful to define certain combinations of rate constants in order to express them concisely.

Recalling the definitions of the rate constants for entry to the channel given in Eq. 4, denoting by μ the rate constants for exit and by λ those for crossing the central barrier, we shall define

$$\bar{K}''^{Ca}_{Ca} = \frac{\bar{\rho}''^{Ca}_{Ca}}{\bar{\mu}'^{Ca}_{Ca}}; \qquad \bar{K}''^{Na}_{Ca} = \frac{\bar{\rho}''^{Na}_{Ca}}{\bar{\mu}'^{Na}_{Ca}}; \qquad \bar{K}'^{Ca}_{Na} = \frac{\bar{\rho}'^{Ca}_{Na}}{\bar{\mu}''^{Ca}_{Na}}$$

$$\bar{\Lambda}''_{Ca} = \frac{\bar{\lambda}''_{Ca}}{\bar{\lambda}'_{Ca}}; \qquad \bar{\Lambda}'_{Na} = \frac{\bar{\lambda}'_{Na}}{\bar{\lambda}''_{Na}}, \quad (6)$$

where the $\bar{K}$s have the obvious meaning of binding constants of the sites in the channel. With the aid of these definitions, the first five parameters in Eq. 5 are given by

$$P_1 = \frac{\bar{\mu}'^{Na}_{Na}}{\bar{\mu}''^{Na}_{Na}}; \qquad P_2 = \frac{\bar{\mu}'^{Ca}_{Ca}}{\bar{\mu}''^{Ca}_{Ca}} \cdot \frac{\bar{\lambda}'_{Ca}}{\bar{\lambda}'_{Ca} + \bar{\rho}''^{Ca}_{Ca} C''_{Ca}}$$

$$P_3 = \frac{\bar{\Lambda}''_{Ca}}{1 + \bar{\Lambda}''_{Ca}} \cdot \frac{\bar{\rho}''^{Ca}_{Ca} C''_{Ca}}{\bar{\lambda}'_{Ca} + \bar{\rho}''^{Ca}_{Ca} C''_{Ca}} \left(\frac{\bar{\lambda}'_{Ca}}{\bar{\mu}''^{Ca}_{Ca}} - 1\right) \quad (7)$$

$$P_4 = \frac{\bar{K}'^{Ca}_{Na}}{1 + \bar{\Lambda}''_{Ca}}; \qquad P_5 = \frac{1 + \bar{\Lambda}'_{Na}}{1 + \bar{\Lambda}''_{Ca}} \cdot \frac{\bar{K}'^{Ca}_{Na}}{\bar{K}''^{Na}_{Ca}}.$$

The meaning of the other two parameters in the numerator of Eq. 5, P_6 and P_7, is slightly less simple. In fact, since the fitted data represent currents normalized to

their reference values, denoted by I^{ref} (peak value of the inward current, found to occur at about −30 mV), one can see that the definition of P_6 and P_7 must include such values. Denoting by p^{ref} and i^{ref} the reference values of the open channel probability and of the single channel current, respectively, and by N^T the total number of channels, I^{ref} will be

$$I^{ref} = N^T p^{ref} i^{ref}, \tag{8}$$

its explicit expression being given by Eq. 11A in the Appendix. If p^M is the maximum value of the open channel probability, and if we assume that this is its actual value in the whole range of positive voltages where we fit the data, P_6 and P_7 are:

$$P_6 = \frac{N^T p^M e}{|I^{ref}|} \cdot \frac{\bar{K}'^{Ca}_{Na}\,\bar{\rho}''^{Na}_{Na}}{\bar{K}'^{Ca}_{Ca}\,(1 + \bar{\Lambda}''_{Ca})}; \qquad P_7 = 2\,\frac{N^T p^M e}{|I^{ref}|} \cdot P_2 \cdot \frac{\bar{\Lambda}''_{Ca}\bar{K}'^{Ca}_{Ca}\bar{\mu}''^{Ca}_{Ca}}{1 + \bar{\Lambda}''_{Ca}}, \tag{9}$$

where e is the unit charge. Although the physical meaning of most of these parameters is not directly intuitive, we shall see later in the Discussion that they provide interesting information about certain features of the channel.

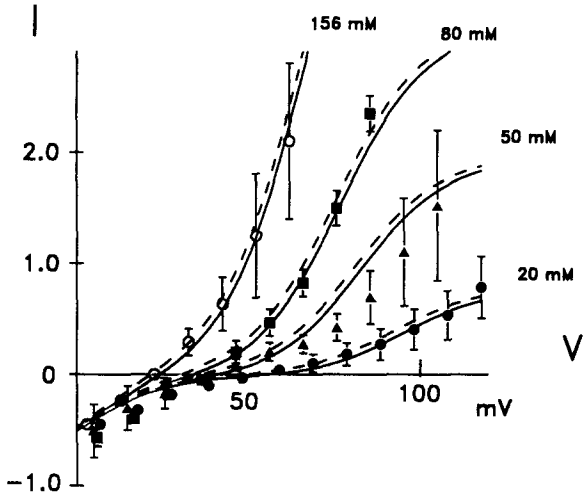

FIGURE 10. Comparison between the model and the data. Continuous curves illustrate the theoretical fits with Eq. 1 in the range of positive voltages using the standard extracellular medium and different intracellular Na^+ concentrations (same as in Fig. 4). The best fitting values for parameters were; P_1 = 25.552, P_2 = 0.0929, P_3 = 0.888, P_4 = 3.837 × 10^{-4} M^{-1}, P_5 = 6.0126 × 10^{-5}, P_6 = 0.063 M^{-1}, P_7 = 52.83 M^{-1}, C''_{Na} = 0.130 M, and C''_{Ca} = 0.0025 M. Symbols and bars are the same as in Fig. 6. Open circles refer to 156 mM $[Na^+]_p$, solid squares to 80 mM $[Na^+]_p$, solid triangles to 50 mM $[Na^+]_p$, and solid circles to 20 mM $[Na^+]_p$. Dashed curves indicate the expected *I-V* relationships in the Na^+-free extracellular medium (C''_{Na} = 0) using the same values for parameters.

Comparison of the Model with the Data

Fig. 10 illustrates the fit of Eq. 5 to the *I-V* data for positive membrane potentials. Since the probability of channel opening is presumably maximal in that range of voltages, and the number of open channels is therefore constant, the shape of the *I-V* curves is expected to reflect only the permeation properties of the channel and not those of gating. The four continuous curves and the four sets of data correspond

to different concentrations of internal sodium, with the external ion composition being constant: 2.5 mM Ca^{2+} and 130.3 mM Na^+. The fit is quite satisfactory, except for the case of 50 mM internal sodium, where deviations are appreciable. Also in this case, however, the theoretical points are within the errors of most of the data. A limitation of the model, to be discussed in more detail later, can be noted in the tendency of the theoretical curves to saturate at high positive potentials, a feature that is not borne out by the average values of the data, although the error bars are sufficiently large that saturating currents can be accommodated within their limits.

The fitting values of the seven parameters, obtained using a "least-square minimization" routine for nonlinear functions, are listed in the legend of Fig. 10. The closeness of the fit was very sensitive to displacements of the parameters from their optimal values, except for the case of P_4.

The dashed curves in Fig. 10 are the currents predicted by the model when the external Na^+ is set equal to zero in Eq. 5 and the values of the parameters are those deduced by fitting the data. The closeness of these curves to the continuous ones demonstrates that, for the values of the parameters deduced from the fit, the theoretically expected sensitivity of the current to changes in external Na^+ is very small. This is in agreement with the results of several experiments, only part of which are illustrated in Fig. 8.

The theoretical dependence of the reversal potential on the Na^+ concentration in the pipette, $[Na^+]_p$, can be calculated by setting the parenthesized quantity in Eq. 5 equal to zero. Using the parameters determined by fitting the *I-V* data, the reversal potential as a function of $[Na^+]_p$ is illustrated by the solid curve in Fig. 5. As can be seen, the fit to the data is quite good.

DISCUSSION

Assumptions of the Model

The channel is never empty of ions. Several early studies with Ca channels have demonstrated that in standard ionic conditions the inward current is an increasing function of the external Ca^{2+} concentration, saturation occurring in the range between 10 and 30 mM (Hagiwara and Takahashi, 1967; Hagiwara and Byerly, 1981). However, recent studies of the effects of monovalent cations on the inward current have also shown that Ca^{2+} ions bind to Ca^{2+} channels very strongly, suggesting the presence of a site (or sites) with a dissociation constant of <1 μM (Almers and McCleskey, 1984). One obvious way to resolve the apparent conflict between these observations has been to propose that Ca channels are multi-ion channels, an idea that has now gained wide acceptance. In consonance with this hypothesis, the weaker binding in the millimolar range, originally reported by Hagiwara and Takahashi (1967), would be related to the channel interaction with the second Ca^{2+} ion.

Capitalizing on the evidence that Ca channels are multi-ion pores with very strong binding sites for Ca^{2+}, we have used a modified version of the "single file" model previously formulated by Urban and Hladky (1979), assuming that the channel is never empty of ions when the ionic conditions are similar to those of our experiments. According to this hypothesis, when the membrane potential is negative (or not too positive with respect to resting), the channel will always contain at least

one Ca^{2+} ion, and the flow of inward current will occur via Ca^{2+} ions hopping into singly occupied channels and out of doubly occupied ones, thus never leaving them empty. However, as the potential is increased to more positive values, Na^+ ions from the cytoplasm will be driven into channels that contain one Ca^{2+} in the site close to the extracellular bath, and will eventually expel this ion from the pore, thus unblocking it and permitting the onset of outward Na^+ fluxes. Note that, for consistency with the assumption that the channel is never empty, states of the channel with two Na^+ ions must be included in the kinetics if outward fluxes of this ion are to be possible at all. It is pleasing, however, that this feature of the kinetics that must be evoked for logical consistency is also required in order to fit both the quadratic dependence of the outward current on the concentration of internal Na^+, $[Na^+]_p$, and the steep dependence of the current on voltage at high $[Na^+]_p$ values. Simpler models for one-ion channels based on Eyring theory would not account for these characteristics of the data, nor would "continuum" treatments based on the Nernst-Planck equation with the approximation of constant field.

Can the doubly occupied state of the channel with Ca^{2+} inside and Na^+ outside be neglected? As we stated earlier in the Results, when the extracellular Ca^{2+} was in the millimolar range, changes in the concentration of external Na^+, $[Na^+]_o$, had almost no effect on either the reversal potential or the current, inward or outward. However, the theoretical results of the general model (not shown in this paper) indicate that effects of external Na^+, $[Na^+]_o$, should be apparent if the probability of state 9 of the channel in Fig. 9 *B* (with Ca^{2+} in the cytoplasmic site and Na^+ in the other) were significantly different from zero. In this case, for example, the inward current would be expected to sense changes of $[Na^+]_o$. Even if a Na^+ from outside were to jump into the channel only to be bounced back by a Ca^{2+} "plug" already present in the cytoplasmic site (therefore without contributing directly to the current), any change in the probability of state 9 caused by changing $[Na^+]_o$ would alter in the opposite direction the probability of state 4, the state with two Ca^{2+} ions considered crucial for the flow of inward current, and would in this way alter the properties of this current. However, although state 9 is likely to play a negligible role when the current flows in the outward direction, this claim should be mitigated in the case of the inward current through L-type Ca^{2+} channels of skeletal muscle. Using this preparation, the peak of the inward current observed when Na^+ was replaced by TEA was somewhat larger than that observed when Na^+ was present and TEA absent (Almers et al., 1984), an effect which, in principle, may be related to Na^+ entry into the channel and formation of state 9.

While the above arguments are deduced a posteriori from the experimental results, there are also other reasons why the probability of state 9 would be expected to be small compared with that of all of the other doubly occupied states of the channel (states 4, 7, and 8 in Fig. 9 *B*). For example, examining the kinetic pathways that lead to formation of states 9 and 4 (the latter being the state with two Ca^{2+} ions in the channel), the following considerations seem plausible: since the Ca^{2+} level in the cytoplasm is extremely low (and so is the chance that a Ca^{2+} ion will enter a channel from inside), it is obvious that the last kinetic steps that lead to the formation of state 9 or state 4 can only be the entry of an external ion (Na^+ or Ca^{2+}, respectively) into a channel that is already in state 2; namely, a channel with one Ca^{2+} ion located in the cytoplasmic site, having arrived there from the external solution.

While it is equally possible for an external Ca^{2+} or Na^+ to enter a channel that is in state 2, the high affinity of the channel for Ca^{2+} makes it reasonable to expect that a Ca^{2+} ion, once bound, will reside in the channel longer than a Na^+, and thus that the time-averaged probability of state 4 will be greater than that of state 9.[1]

In addition, there are also valid reasons why state 9 would be expected to occur less frequently than the other two doubly occupied states of the channel with Na^+, states 7 and 8. Both the latter, in fact, can form via Na^+ ions entering the channel from the cytoplasmic side, where the competition with Ca^{2+} for getting into the channel is negligible, whereas state 9, as we argued above, can only form via Na^+ ions entering from outside, where the competition with Ca^{2+} is very great.

For all these reasons we have considered it justifiable to simplify our treatment by neglecting the contribution of state 9 to the kinetics.

Location in the field of the energy peaks and wells. The fit depended crucially on the "electrical" position of the peaks and wells of the energy barriers. The configuration of the channel that intuitively would seem to be the most probable (insofar as it is consistent with minimal repulsion between the cations in doubly occupied channels), is the one with the two sites close to the two opposite interfaces. However, this configuration was clearly inadequate to fit all the four *I-V* curves, the main reason being that it implies lack of voltage dependence for the rate constants for exit to the external solution. Similarly inadequate were energy profiles with evenly spaced peaks and wells, as well as models in which the dependence on the voltage was given only to the rate constants for movement in one of the two directions, outward or inward (sawtooth-shaped profiles). Instead, a good fit could be obtained assuming electrical proximity of both of the two sites to the cytoplasmic medium, implying that the entire "transmembrane" voltage drops between the site close to the external medium and the outer mouth of the channel and, consequently, that only the rate constants for exit to the external medium, μ', and those for entry from that medium, ν'', can be voltage dependent. However, to comply with recently obtained evidence, which indicates that the kinetics of Ca^{2+} entry from outside is insensitive to voltage (Lansman et al., 1986), the peak of the outermost barrier was assumed to be adjacent to the outer mouth of the channel, so that only the rate constants for exit to the external solution (and not those for entry from that solution) are functions of the voltage. A potential profile of this type could be explained if the inner segment of the pore, comprising its cytoplasmic end and both of the two sites, could be regarded as a polar, high dielectric medium. In this case, electrical proximity of the two sites would not necessarily imply physical closeness. In principle, however, even physical closeness between the two sites may be conceivable if they are constituted of highly charged negative groups. Rosenberg et al. (1986) have shown that Ca^{2+} channels from cardiac sarcolemmal vesicles, when incorporated in lipid bilayers and interposed between symmetric solutions of 100 mM $BaCl_2$ and 50 mM NaCl, exhibit a nearly perfect ohmic behavior up to >100 mV. This feature would be difficult to reconcile with our model, whereas it would be consistent with a more symmetric

[1]What is said here should not be construed to imply that the effects of external Na^+ have been neglected altogether. This would violate "microscopic reversibility" and the second law. In our kinetic scheme, external Na^+ is allowed to contribute to the formation of state 7 (the state of the channel with two Na^+), and the condition $\bar{\rho}'^{Na}_{Na}\bar{\lambda}'_{Na}\bar{\mu}'^{Na}_{Na} = \bar{\rho}''^{Na}_{Na}\bar{\lambda}''_{Na}\bar{\mu}''^{Na}_{Na}$, which is imposed by microscopic reversibility, is used to deduce Eq. 10A and Eq. 5 from Eq. 6A.

energy profile. On the other hand, such a symmetric profile would be unfit to explain the strong rectification and the steep increase of the outward current with voltage observed by those authors in the same channel when Ba^{2+} is removed from the internal solution. Since this behavior in asymmetric conditions is qualitatively similar to that observed with our channel, it is very likely that a model similar to ours would account for it. Although the reason for this inconsistency is not clear, it may be related to drastic effects on the characteristics of the permeation pathway of the channel induced by the presence of high concentrations of divalent cations in the internal solution.

As can be seen in Fig. 10, the theoretical curves saturate at high voltages, a trend not shown by the averaged values of the data (although the error bars are sufficiently wide to allow saturating curves within their limits). This behavior is due to the fact that, consistent with the chosen positions for the barrier peaks in the field, the rate constant for Na^+ entry from the cytosolic solution is independent of voltage. Different energy profiles, which allowed a significant voltage dependence for that constant, drastically impaired the overall fit.

Although the reason for this discrepancy is not clear, it may be related to field-induced distortions of the channel structure, and thus of the energy profile (such, for example, that the rate constant for Na^+ entry would become increasingly voltage dependent as the applied field is raised to positive values). However, to minimize the number of assumptions, we have preferred to use a model that does not have the flexibility to allow for these complexities.

What Can Be Learned about the Channel from the Parameters?

The simplest of the parameters, P_1, represents the ratio of the two rate constants for Na^+ exit from the channel when both sites are occupied by sodium. The fact that its value is greater than one (~25) indicates that it is easier for a Na^+ in a Ca channel to move out of the channel to the external medium than to the cytoplasm.

Interesting information can be also deduced from P_3. From its value (−0.89) and from Eq. 7, where P_3 is expressed as the product of three factors, it can be deduced via simple reasoning that the absolute value of each of those factors must be between 0.89 and 1. This clearly implies

$$\bar{\lambda}'_{Ca} < \bar{\lambda}''_{Ca}; \qquad \bar{\lambda}'_{Ca} < \bar{\rho}''^{Ca}_{Ca} C''_{Ca}; \qquad \bar{\lambda}'_{Ca} < \bar{\mu}''^{Ca}_{Ca}. \tag{10}$$

Taken together, these three relations suggest that λ'_{Ca}, the rate constant for Ca^{2+} movement across the central barrier in the outward direction, is a small quantity, making it difficult for Ca^{2+} to move in such a direction. Moreover, a consequence of the first of the above inequalities, $\lambda'_{Ca} < \lambda''_{Ca}$, is that the site that binds Ca^{2+} most strongly is the one nearest to the cytoplasmic solution (in both singly and doubly occupied channels). In fact, using microscopic reversibility, it can be easily shown that

$$\frac{\bar{\lambda}''_{Ca}}{\bar{\lambda}'_{Ca}} = \frac{\bar{K}'_{Ca}}{\bar{K}''_{Ca}} = \frac{\bar{K}'^{Ca}_{Ca}}{\bar{K}''^{Ca}_{Ca}}. \tag{11}$$

Since $\lambda'_{Ca}/\lambda''_{Ca} < 1$ (see the first inequality in Eq. 10), it follows that $K'_{Ca} > K''_{Ca}$ and $K'^{Ca}_{Ca} > K''^{Ca}_{Ca}$.

From P_2 and P_3 it is also possible to infer the upper limit for the binding constant K''^{Ca}_{Ca} relative to the binding of the second Ca^{2+} ion by the site close to the extracellular solution. Using the approximation $\bar{\lambda}'_{Ca} + \bar{\rho}''^{Ca}{}_{Ca}C''_{Ca} \simeq \bar{\lambda}'_{Ca}$, justifiable on account of the second inequality in Eq. 10, and recalling the definition of K''^{Ca}_{Ca} in Eq. 6, the expression that defines P_2 in Eq. 7 can be rewritten in the form

$$\bar{K}''^{Ca}_{Ca} \simeq \frac{\bar{\lambda}'_{Ca}}{\bar{\mu}''^{Ca}_{Ca}} \cdot \frac{1}{P_2 C''_{Ca}}. \tag{12}$$

On the other hand, as a corollary of the above discussion about P_3,there follows also that the ratio $\bar{\lambda}'_{Ca}/\bar{\mu}''^{Ca}_{Ca}$, which appears in that definition of P_3 in Eq. 7, cannot be greater than 0.11. Inserting this limiting value in Eq. 12, along with the values for P_2 (= 0.09) and C''_{Ca} (0.0025 M), one finds that $K''^{Ca}_{Ca} < 490\ M^{-1}$, or, equivalently, that the dissociation constant, K_d (= $1/K''^{Ca}_{Ca}$), must be greater than 2.0 mM. This is consistent with the fact that saturation of the inward current at millimolar levels of Ca^{2+}, probably due to binding of the second Ca^{2+} ion by the channel, occurs at concentrations higher than 2.0 mM, generally between 10 and 30 mM (Hagiwara and Byerly, 1981).

Finally, from P_7 it is possible to deduce the ratio between the maximum value for the open channel probability, p^M (presumably coinciding with its actual value at positive membrane potentials) and its corresponding value at the peak of the inward current (reference value, corresponding to a membrane potential of about −30 mV). In fact, substituting the explicit expression for I^{ref}, Eq. 11A, in the definition of P_7, (Eq. 9), and rearranging, one finds

$$\frac{p^M}{p^{ref}} = \frac{P_7 C'_{Ca}}{1 + P_2 e^{2\phi ref} + P_3}. \tag{13}$$

Using the fitting values for P_7 (= 52.8 M^{-1}), P_2 (= 0.09), and P_3 (= −0.89), p^M/p^{ref} is found to be ~1.1, suggesting that about 90% of the functional channels are already open at the reference potential (about −30 mV).

APPENDIX

A Two-Site, Two-Ion Model for a Channel: Derivation of Eq. 5

A two-site, single-file pore can exist in any of the nine states of Fig. 9 *B* if Ca^{2+} and Na^+ ions are both permeant. However, for reasons discussed in the text, we have neglected both state 1 and state 9, thus reducing the number of possible states of occupancy of the channel from nine to seven. In this case, seven kinetic equations can be written to express the fact that, at a steady state, the net rate of formation of each of those states must vanish. For example, for state 2 we will have

$$\frac{dP_2}{dt} = \lambda''_{Ca}P_3 - \lambda'_{Ca}P_2 + \mu'^{Ca}_{Ca}P_4 - \nu''^{Ca}_{Ca}P_2 = 0, \tag{1A}$$

and analogous relations can be written for the other six states. However, since only six of the seven equations thus obtained are independent, an additional relation is required to calculate the seven unknown probabilities, the simplest one being the normalization of the sum of the probabilities to one. Once P_2, P_3, P_4, and P_5 are calculated, substitution in Eqs. 1 and 2 yields explicit expressions for the fluxes of Ca^{2+} and Na^+, and hence for the current.

For brevity, and also to render the equations more easily comprehensible, it is useful to group certain recurring combinations of rate constants. Recalling the notation used for the various rate constants (Eqs. 3 and 4), we shall define:

$$\Omega'_{Na} = \nu'^{Na}_{Na}\mu'^{Na}_{Na} + \lambda''_{Na}(\mu'^{Na}_{Na} + \mu''^{Na}_{Na}); \quad \Omega''_{Na} = \nu''^{Na}_{Na}\mu''^{Na}_{Na} + \lambda'_{Na}(\mu'^{Na}_{Na} + \mu''^{Na}_{Na})$$
$$\Omega''_{Ca} = \nu''^{Ca}_{Ca}\mu''^{Ca}_{Ca} + \lambda'_{Ca}(\mu'^{Ca}_{Ca} + \mu''^{Ca}_{Ca}) \tag{2A}$$

$$P = \Omega'_{Na} + \Omega''_{Na} + \lambda'_{Na}\nu'^{Na}_{Na} + \lambda''_{Na}\nu''^{Na}_{Na} + \nu'^{Na}_{Na} + \nu''^{Na}_{Na}$$
$$\Omega = \nu'^{Ca}_{Na}\mu'^{Na}_{Ca}P + \Omega'_{Na}\nu''^{Na}_{Ca}(\nu'^{Ca}_{Na} + \mu''^{Ca}_{Na}) \tag{3A}$$

$$\Delta = \Omega''_{Ca}\Omega + \Omega'_{Na}\lambda''_{Ca}\mu''^{Ca}_{Na}\nu''^{Na}_{Ca}(\mu'^{Ca}_{Ca} + \mu''^{Ca}_{Ca} + \nu''^{Ca}_{Ca}). \tag{4A}$$

The fluxes of Ca^{2+} and Na^+ (expressed in moles per second per channel) can now be written

$$j_{Ca} = -\frac{\Omega'_{Na}\lambda''_{Ca}\mu''^{Ca}_{Na}\mu''^{Ca}_{Ca}\rho''^{Ca}_{Ca}C''^{2}_{Ca}}{\Delta} \tag{5A}$$

$$j_{Na} = \frac{\Omega''_{Ca}\mu''^{Na}_{Ca}\rho'^{Ca}_{Na}C'_{Na}(\rho'^{Na}_{Na}\lambda'_{Na}\mu'^{Na}_{Na}C'_{Na} - \rho''^{Na}_{Na}\lambda''_{Na}\mu''^{Na}_{Na}C''_{Na})}{\Delta}. \tag{6A}$$

At this stage, a reasonable approximation is suggested by our experimental finding that the current, at given positive voltages, increases approximately as the square power of the internal Na^+ concentration, C'_{Na} (or $[Na^+]_p$) (see Fig. 7). In accordance with this, the equation for the flux of Na^+, Eq. 6A, indeed contains a term in the numerator that is proportional to the square power of C'_{Na}. However, since the quadratic dependence must be a property of the whole expression for the flux (and not only of its numerator) to be consistent with the data, it is clear that the wole denominator must not be proportional to C'_{Na}, nor must its terms with high powers of C'_{Na} significantly affect its value when C'_{Na} is varied in the range of our experiments. From analysis of Eqs. 2A–6A, one can see that these requirements are met if it is assumed that the rates for Na^+ ion entry into channels already occupied by one Na^+, ν'^{Na}_{Na} and ν''^{Na}_{Na}, are smaller than the rate constants for jumping across the central barrier, λ'_{Na} and λ''_{Na} (in singly occupied channels), as well as smaller than the rate constants for jumping out of doubly occupied channels, μ'^{Na}_{Na} and μ''^{Na}_{Na}. These approximations are also intuitively plausible, considering that the entry of Na^+ ions into channels with a site occupied by another Na^+ will be hindered by electrostatic interaction with the ion already present in the channel. Thus, using these simplifications, we will have

$$\Omega'_{Na} \simeq \lambda''_{Na}(\mu'^{Na}_{Na} + \mu''^{Na}_{Na}); \quad \Omega''_{Na} \simeq \lambda'_{Na}(\mu'^{Na}_{Na} + \mu''^{Na}_{Na})$$
$$P \simeq (\lambda'_{Na} + \lambda''_{Na})(\mu'^{Na}_{Na} + \mu''^{Na}_{Na}) \tag{7A}$$
$$\Omega \simeq (\mu'^{Na}_{Na} + \mu''^{Na}_{Na})[\nu'^{Na}_{Ca}\mu'^{Na}_{Ca}(\lambda'_{Na} + \lambda''_{Na}) + \lambda''_{Na}\nu''^{Na}_{Ca}(\nu'^{Ca}_{Ca} + \mu''^{Ca}_{Na})],$$

and Δ, the denominator of the fluxes in Eqs. 5A and 6A, becomes

$$\Delta \simeq \Omega''_{Ca}(\mu'^{Na}_{Na} + \mu''^{Na}_{Na})\left\{\lambda''_{Ca}\nu''^{Na}_{Ca}\left[\nu'^{Ca}_{Na} + \mu''^{Ca}_{Na} + \lambda''_{Na}\mu''^{Ca}_{Na}\frac{\mu'^{Ca}_{Ca} + \mu''^{Ca}_{Ca} + \nu''^{Ca}_{Ca}}{\Omega''_{Ca}}\right] + \nu'^{Ca}_{Na}\mu'^{Na}_{Ca}(\lambda'_{Na} + \lambda''_{Na})\right\}. \tag{8A}$$

Recalling that the total cell membrane current for positive potentials is

$$I = N^{T} p^{M} e(j_{Na} + 2j_{Ca}), \tag{9A}$$

where N^{T} is the total number of channels and p^{M} is open-channel probability for positive membrane potentials, an explicit expression for the current as a function of the concentrations can be obtained by combining Eq. 9A with Eqs. 5A, 6A, and 8A. Finally, choosing the positions for the sites and the barrier peaks as specified in the paper, (such that only the rate constants for exit from the pore to the external medium are voltage dependent), the equation for the current becomes an explicit function also of the voltage, namely,

$$I = N^{T} p^{M} e \left\{ \frac{\dfrac{\overline{K}''^{Ca}_{Na}}{\overline{K}''^{Na}_{Ca}} \cdot \dfrac{\overline{\rho}''^{Na}_{Na} e^{2\phi}}{1 + \overline{\Lambda}''_{Ca}} \cdot C'_{Na}(C'_{Na} e^{\phi} - C'_{Na})}{1 + P_1 e^{\phi}} - \frac{2P_2 \cdot \dfrac{\overline{\Lambda}''_{Ca}}{1 + \overline{\Lambda}''_{Ca}} \cdot \overline{\mu}''^{Ca}_{Ca} \overline{K}''^{Ca}_{Ca} C''^{2}_{Ca}}{1 + P_2 e^{2\phi}} \right\}$$

$$\times \frac{1}{C''_{Ca}\left(1 + \dfrac{P_3}{1 + P_2 e^{2\phi}}\right) + (P_4 C''_{Ca} + P_5 e^{2\phi}) C'_{Na}}, \tag{10A}$$

where the five parameters, P_1–P_5, have been defined in Eq. 7. To obtain Eq. 5, which is the equation used to fit the data, and which corresponds to the current normalized to its reference value (maximum negative value), we must calculate such reference current and divide Eq. 10A by its absolute value. Realizing that at the reference potential (−30 mV) the current is carried mainly by Ca^{2+} ions, we shall deduce from Eq. 10A

$$I^{ref} \simeq N^{T} p^{ref} e \frac{-2P_2 \cdot \dfrac{\overline{\Lambda}''_{Ca}}{1 + \overline{\Lambda}''_{Ca}} \cdot \overline{\mu}''^{Ca}_{Ca} \overline{K}''^{Ca}_{Ca} C''^{2}_{Ca}}{1 + P_2 e^{2\phi ref}} \cdot \frac{1}{C''_{Ca}\left[1 + \dfrac{P_3}{1 + P_2 e^{2\phi ref}}\right]}, \tag{11A}$$

where ϕ^{ref} denotes the reference potential and p^{ref} is the corresponding open-channel probability at that potential. Thus, dividing Eq. 10A by Eq. 11A, and recalling the definitions of the parameters P_6 and P_7 given in Eq. 9, one finally obtains the normalized expression for the current, Eq. 5.

We thank Dr. Y. Kidokoro and R. L. Byerly for valuable comments and suggestions.

The work was supported by United States Public Health Service grant NS-09012 and by grants from the Muscular Dystrophy Association to Dr. S. Hagiwara and Dr. S. Ciani.

Original version received 28 April 1989 and accepted version received 16 April 1990.

REFERENCES

Almers, W., and E. W. McCleskey. 1984. Non-selective conductance in calcium channels of frog muscles: calcium selectivity in a single-file pore. *Journal of Physiology.* 353:585–608.

Almers, W., E. W. McCleskey, and P. T. Palade. 1984. A non-selective cation conductance in frog muscle membrane blocked by micromolar external calcium ions. *Journal of Physiology.* 353:565–584.

Byerly, L., P. B. Chase, and J. R. Stimers. 1985. Permeation and interaction of divalent cations in calcium channels of snail neurons. *Journal of General Physiology.* 85:491–518.

Campbell, D. L., W. R. Giles, and E. F. Shibata. 1988. Ion transfer characteristics of the calcium current in bull-frog myocytes. *Journal of Physiology.* 403:239–266.

Fenwick, E. M., A. Marty, and E. Neher. 1982. Sodium and calcium channels in bovine chromaffin cells. *Journal of Physiology.* 311:599–635.

Fukushima, Y., and S. Hagiwara. 1985. Current carried by monovalent cations through calcium channels in mouse neoplastic B lymphocytes. *Journal of Physiology.* 358:255–284.

Fukushima, Y., S. Hagiwara, and R. E. Saxton. 1984. Variation of calcium current during the cell growth cycle in mouse hybridoma lines secreting immunoglobulins. *Journal of Physiology.* 355: 313–321.

Hagiwara, S., and L. Byerly. 1981. Calcium channel. *Annual Review of Neuroscience* 4:69–125.

Hagiwara, S., and H. Ohmori. 1982. Studies of calcium channels in rat clonal pituitary cells with patch electrode voltage clamp. *Journal of Physiology.* 331:231–252.

Hagiwara, S., S. Ozawa, and O. Sand. 1975. Voltage clamp analysis of two inward current mechanisms in the egg cell membrane of a starfish. *Journal of General Physiology.* 65:617–644.

Hagiwara, S., and K. Takahashi. 1967. Surface density of calcium ions and calcium spikes in the barnacle muscle fiber membrane. *Journal of General Physiology.* 50:583–601.

Hess, P., and R. W. Tsien. 1984. Mechanism of ion permeation through calcium channels. *Nature.* 309:453–456.

Hille, B., and W. Schwarz. 1978. Potassium channels as multi-ion single-file pores. *Journal of General Physiology.* 72:409–442.

Iijima, T., S. Ciani, and S. Hagiwara. 1986. Effects of the external pH on Ca channels: experimental studies and theoretical considerations using a two-site, two ion model. *Proceedings of the National Academy of Science USA.* 83:654–658.

Kostyuk, P. G., and O. A. Krishtal. 1977. Effects of calcium and calcium-chelating agents on the inward and outward current in the membrane of mollusc neurones. *Journal of Physiology.* 270:569–580.

Kostyuk, P. G., and S. L. Mironov. 1986. Some predictions concerning the calcium channel model with different conformational states. *General Physiology and Biophysics.* 6:649–659.

Kostyuk, P. G., S. L. Mironov, and M. Y. Shuba. 1983. Two ion-selecting filters in the calcium channel of the somatic membrane of mollusc neurons. *Journal of Membrane Biology.* 76:83–93.

Lansman, J. B., P. Hess, and R. W. Tsien. 1986. Blockade of current through single calcium channels by Cd^{2+}, Mg^{2+}, and Ca^{2+}. *Journal of General Physiology.* 88:321–347.

Narahashi, T., A. Tsunoo, and M. Yoshii. 1987. Characterization of two types of calcium channels in mouse neuroblastoma cells. *Journal of Physiology.* 383:231–249.

Nowycky, M. C., A. P. Fox, and R. W. Tsien. 1985. Three types of neuronal calcium channel with different calcium agonistic sensitivity. *Nature.* 316:440–443.

Reuter, H., and H. Scholz. 1977. A study of ion selectivity and kinetic properties of the calcium dependent slow inward current in mammalian cardiac muscle. *Journal of Physiology.* 264:17–47.

Rosenberg, R. L., P. Hess, J. P. Reeves, H. Smilowitz, and R. W. Tsien. 1986. Calcium channels in planar bilayers: Insights in mechanisms of ion permeation and gating. *Science.* 231:1564–1566.

Urban, B. W., and S. B. Hladky. 1979. Ion transport in the simplest single file pore. *Biochimica et Biophysica Acta.* 554:410–429.

Yamashita, N., S. Ciani., and S. Hagiwara. 1989. Effect of internal Na ions on the outward current through the Ca channels in mouse neoplastic B lymphocytes. *Biophysical Journal.* 55:596*a*. (Abstr.)